Ion Heating and Acceleration by Strong Magnetosonic Waves

B. Lembege,[a] S. T. Ratliff,[b] J. M. Dawson, and Y. Ohsawa[c]
Department of Physics, University of California, Los Angeles, Los Angeles, California 90024
(Received 21 March 1983)

Large-amplitude magnetosonic waves ($\vec{k}\perp\vec{B}$) with $\omega_{ci}<\omega<\omega_{lh}$ (ω_{ci} and ω_{lh} are the ion-cyclotron and lower-hybrid frequencies) are investigated by particle simulation. Some ions are accelerated and trapped in the potential troughs of the waves; the $\vec{v}\times\vec{B}/c$ force accelerates these particles parallel to the phase fronts. Ultimately, the $\vec{v}\times\vec{B}/c$ force detraps the ions but only when $\vec{v}$ is much larger than the Alfvén velocity; the wave is strongly damped by this effect.

PACS numbers: 52.50.Gj, 52.35.Dm, 52.60.+h, 52.65.+z

Many different types of waves have been considered for plasma heating in fusion devices. Although magnetosonic waves, primarily in the form of shock waves in theta pinches, have been considered, they have generally not been taken into account as a serious contender. Magnetosonic waves, also in the form of shocks, have been studied more extensively in connection with the Earth's bow shock and its structure. Ion heating in the Earth's bow shock was treated analytically during the 1970's.[1-4] More recently, a numerical shock model was developed for treating plasma flowing through the rapid magnetic field variation of a shock.[5,6] A hybrid one-dimensional simulation code was used with phenomenological resistive electron heating; then, a longitudinal electric field is obtained only by the requirement of charge neutrality. In this case, most of the incident ions are only moderately heated by compression.[5,6] A fully kinetic two-dimensional code has recently been used to study shock waves generated by a magnetic piston.[7] This code permitted an estimation of both electron and ion heating rates through the shock. However, these various studies did not consider in detail the kinetic charge-separation effects and the associated acceleration and heating mechanisms; they were more devoted to the consequences of the ion reflection and gyration (overshoots in the magnetic field and density profiles).

In this paper we study the acceleration of ions and the associated plasma heating by intense magnetosonic waves (but not shock waves) propagating perpendicular to a magnetic field. While this problem is related to that of magnetosonic shock waves (the limiting case of one sharp magnetic and density jump), it is also different. It elucidates some of the physical phenomena involved in dissipation of intense magnetosonic waves as well as shock waves. As shown a little later, the role of charge spearation is of central importance here, since it governs the trapping conditions of ions; a similar process for electrostatic waves has been considered.[8-10] The present work shows that this effect is of critical importance even when the wave motion is primarily determined by magnetic force. It also shows that for the magnetosonic waves the dominant heating is ion heating; thus treatments of perpendicular shocks which attempt to provide the dissipation through anomalous electron resistivity will give incorrect results. In fusion research great attention is being given to heating of plasmas by lower-hybrid waves which are limiting forms of magnetosonic waves. The present calculations show that if sufficient intensity is used, one is not constrained to the lower-hybrid frequency but can use waves of any lower frequency. Such waves would propagate radially inward more effectively than lower-hybrid waves. If they are properly focused and make use of the variations of the magnetosonic velocity within the plasma, it should be possible to control the region of dissipation to the central region of the plasma.

The present simulations were performed by use of a $1\frac{2}{2}$-dimensional, fully electromagnetic, relativistic particle code with both ions and electrons; standard finite-size particle techniques are used.[11,12] Basically, the code solves the equations

$$\nabla\times\vec{E}=-\frac{1}{c}\frac{\partial\vec{B}}{\partial t},\quad \nabla\times\vec{B}=\frac{1}{c}\frac{\partial\vec{E}}{\partial t}+\frac{4\pi\vec{j}}{c},$$

$$\nabla\cdot\vec{E}=4\pi\rho,\quad \frac{d}{dt}m_{i,e}\dot{\vec{r}}_{i,e}=\pm e\left(\vec{E}+\frac{\vec{v}_{i,e}\times\vec{B}}{c}\right),$$

and the particle charge density ρ and the plasma current j are computed from the particle positions and velocities (e, electrons; i, ions; in the last equation, the plus sign holds for ions and the minus for electrons). One spatial dimension, x, is retained and three velocity and field components are included in the calculation. A static external field B_{0z} is imposed; an external current (j_y not

produced by the plasma) $j_y = j_{0y} \sin(kx - \omega t)$ is applied to drive the wave to ever larger amplitude until nonlinear effects become important; ω is chosen so that $\omega_{ci} < \omega < \omega_{lh}$ where ω_{ci} and ω_{lh} are the ion-cyclotron frequency and the lower-hybrid frequency respectively; k is chosen to satisfy approximately the magnetosonic dispersion relation.

The system length was taken to be much larger than the average ion gyroradius ($L/\rho_i \approx 70$) and the total run time covers a few ion gyroperiods τ_{ci}. The system is allowed to evolve in time and in space; periodic boundary conditions in the x direction are imposed on the particles and fields.

All quantities in the computer code are normalized so that they are dimensionless; here we denote dimensionless variables by a tilde. Specifically, the normalized spatial coordinate is $\tilde{x} = x/\Delta$; velocity $\tilde{v} = v/\omega_{pe}\Delta$, momentum of species α $\tilde{p}_\alpha = p_\alpha/m_\alpha\omega_{pe}\Delta$; electric field $\tilde{E} = eE/m_e\omega_{pe}^2\Delta$; magnetic field $B = eB/m_e\omega_{pe}^2\Delta$; current density $\tilde{j} = j/n_0(\omega_{pe}\Delta)e$; time $\tilde{t} = \omega_{pe}t$. The parameters Δ, ω_{pe}, m_e, e, and n_0 are, respectively, the numerical grid spacing, the electron plasma frequency at $t = 0$, the electron mass, the electric charge, and the particle density at $t = 0$.

The simulations presented here were performed under the following plasma conditions: The length of the system $\tilde{L} = 512$; the particle density per grid point $n_e = n_i = n_0 = 10$ for both electrons (e) and ions (i); the mass and initial temperature ratios are, respectively, $m_i/m_e = 50$ and $T_e/T_i = 1$; the electron thermal speed at $t = 0$ is $\tilde{v}_{tx} = \tilde{v}_{ty} = \tilde{v}_{tz} = 1$; the magnetostatic field is $\tilde{B}_{0x} = \tilde{B}_{0y} = 0$ and $\tilde{B}_{0z} = 10$.

Under these conditions the Alfvén velocity is $\tilde{v}_A = 1.4$, the ion gyroradius is $\tilde{\rho}_i = 7$, and $\tilde{\tau}_{ci} = 314$. The total run time is $\tilde{t}_{end} = 600$ so that $\tilde{t}_{end} \approx 2\tilde{\tau}_{ci}$. The characteristics of the applied current are $\tilde{j}_{0y} = 4$, $\tilde{\omega} = 0.068 = 3.4\tilde{\omega}_{ci}$, and $\tilde{k} = 0.049$, so that the phase velocity $\tilde{v}_p$ of the wave generated by this current is 1.388, approximately equal to $\tilde{v}_A$.

During the early stages of the buildup of the magnetosonic wave, the ion motion is predominantly longitudinal since $\omega \gg \omega_{ci}$ and the ion velocity is small compared to the phase velocity. At later times the longitudinal electric field becomes strong enough to accelerate some ions to its phase velocity. These particles are trapped and strongly interact with the wave whose energy and momentum they absorbed.

The major results can be summarized as follows. Strong acceleration and heating of ions take place once the wave reaches an amplitude where ion trapping takes place ($eE_x/m_i\omega \approx v_p$). This heating is associated with an acceleration of the trapped ions in the y direction due to the $e\vec{v}_p \times \vec{B}/c$ force and it continues until $e\vec{v}_y \times \vec{B}/c$ is large enough to detrap them (approximately E_x). Ion temperatures in the x and y directions, T_{xi} and T_{yi}, show oscillations in time due to the ion-cyclotron motion; the oscillations in T_{yi} are $\pi/2$ out of phase with those in T_{xi}. The heated ions produce a long flat tail on the ion distribution function with a maximum velocity of about 2.5 times the Alfvén velocity. The electrons show negligible heating; they respond adiabatically. The ions acquire a net drift in the y direction $\langle \tilde{v}_{yi} \rangle \approx 0.03$; this drift arises because the wave displaces ions in the x direction and the y momentum, $p_y = m\Delta v_y - eB_0\Delta x/c$, is conserved.

The development of the wave is graphically shown in phase space in Figs. 1 and 2. Figures 1(a) and 1(c) show (x, p_{xi}) at times $t \simeq \tau_{ci}/2$ and τ_{ci}, respectively; each point is the position and momentum of a particle. Figures 1(b) and 1(d) show corresponding (x, p_{yi}) plots. Figures 2(a)–2(d) show (p_{xi}, p_{yi}) plots for $t/\tau_{ci} \simeq \frac{1}{2}$, 1, $\frac{3}{2}$, and 2. At early times [Fig. 1(a)], the ions have a bulk motion due to the presence of the magnetosonic wave; their maximum velocity is less than the Alfvén velocity (the Alfvén momentum is $\tilde{p}_A = 1.43$). At later times, some ions have become trapped in wave troughs and are moving at the

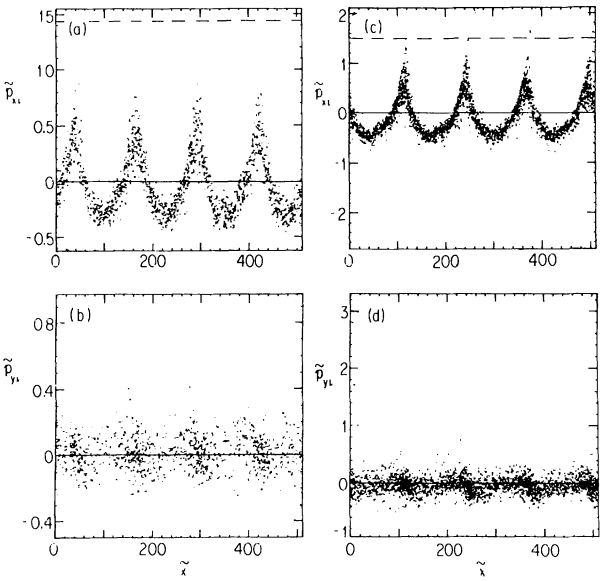

FIG. 1. Ion phase-space plots at (a), (b) $\tilde{t} = 150$ and (c), (d) $\tilde{t} = 300$ vs the space coordinate $\tilde{x}$. The dashed line represents the Alfvén momentum $\tilde{p}_A = 1.43$.

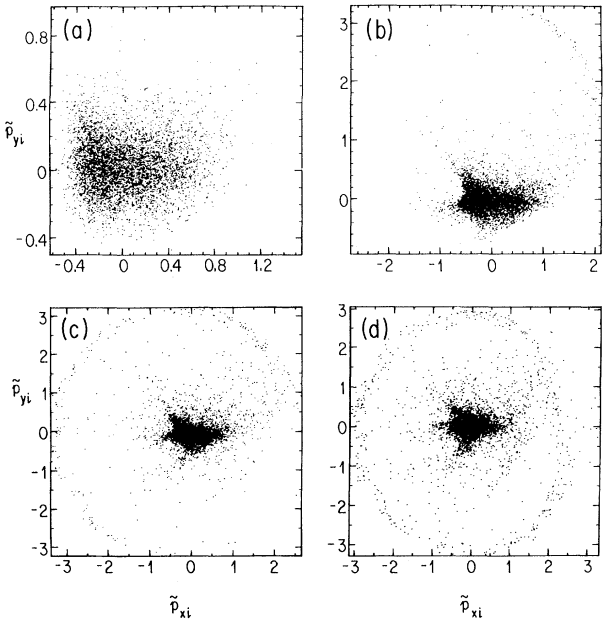

FIG. 2. Ion phase-space plots $(\tilde{p}_{xi}, \tilde{p}_{yi})$ at $\tilde{t} = 150$, 300, 450, and 600. Note the change of scales between plots.

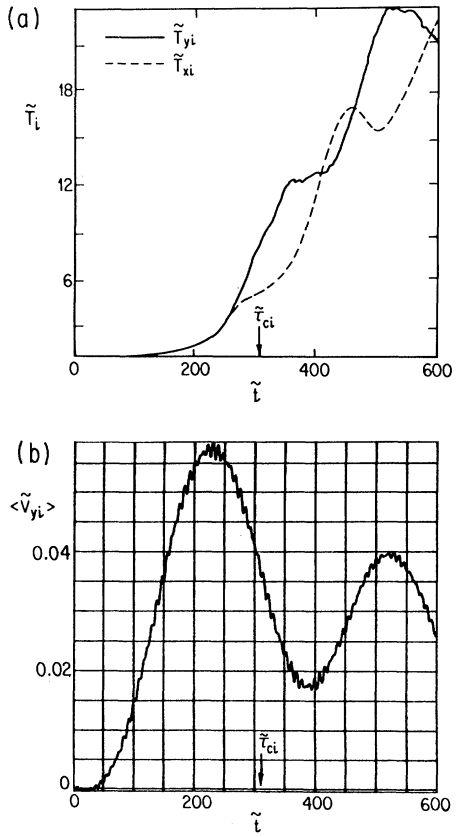

FIG. 3. (a) Local ion temperature vs time, measured along x and y directions. The total length of the model was divided into 32 boxes and inside each box, the local temperature in direction α was calculated by calculating $\langle p_\alpha^2 \rangle - \langle p_\alpha \rangle^2$ (average over all ions in the box). Then all boxes were averaged over. (b) Ion y velocity $\langle \tilde{v}_{yi} \rangle$ averaged over all ions vs time $\tilde{t}$.

Alfvén speed in the x direction. This causes their acceleration in the y direction which is responsible for the large values of p_{yi}, as shown in Fig. 1(d). This acceleration process is shown quite clearly in plots of (p_{xi}, p_{yi}) in Figs. 2(a)–2(d).

Another interesting feature of the trapped particles is shown in Fig. 1(c). For unmagnetized plasmas the trapped particles show a characteristic vortex structure in phase space; this is not the case here. The trapped particles only overshoot the phase velocity by a modest amount and show a small loop in this (x, p_{xi}) diagram. This is because as a trapped particle accelerates parallel to the wave phase fronts, the magnetic force tends to balance out the electric force, and the sloshing motion in the wave troughs is prevented.

Corresponding plots of the ion distribution function, f, exhibit a drift of ions with $p_{xi} < 0$ for early times and the formation of energetic ion tails in both $f(\tilde{p}_{xi})$ and $f(\tilde{p}_{yi})$ for later times; oscillations of the tails due to gyromotion are evident. The heating and gyration effects are displayed in the plots of T_{xi} and T_{yi} shown in Fig. 3(a); the temperatures are the mean ion energies.

There is a continuous feed of particles from the bulk plasma into the trapped region, as shown at different times in Figs. 1 and 2. Since the period of the wave and the cyclotron period are not multiples of each other, there is some stochastic motion in phase space at this time as the particles gyrate; this broadens the band of accelerated ions in Fig. 2. There have been many studies of stochastic heating by waves in a magnetic field.[13] However, here we see mostly nonstochastic (i.e., systematic) heating of the ions.

The wave carries momentum as well as energy. This momentum is transferred to the accelerated particles, i.e., the trapped particles. The trapped particles undergo an x motion; however, they cannot maintain this motion since it requires them to cross the magnetic field B_z. Consequently no steady x motion can exist. The motion in the x direction of the trapped ions gives an x current during their trapping time, and this polarizes the plasma producing an average E_x which gives a drift motion $E_x \times B_z$ along the y direction. The velocity component v_{yi} is plotted versus time in Fig. 3(b); it is seen to build up ($e\vec{v}_p \times \vec{B}/c$ force)

and oscillate about a nonzero value ($\langle \bar{v}_{yi} \rangle \simeq 0.03$). Theoretically, the $\vec{j}_x \times \vec{B}_z/c$ force is just what is required to accelerate the plasma in the y direction as observed in this figure. A nonzero average ion velocity is observed in the y direction since there is a continual supply of ions which can become trapped.

The present results confirm quite well that magnetosonic waves are a good candidate for acceleration and heating of ions in the direction perpendicular to the magnetic field. One point of interest in this mechanism is its selectivity: The electrons are only poorly heated. Although they do not contribute directly to the heating of the plasma, they play an important role through the strong charge-separation effects which play a dominant role in the acceleration and heating mechanisms.

This mechanism is particularly interesting since waves of a broad range of frequencies will work ($\omega_{ci} < \omega < \omega_{lh}$; no resonance is involved) provided that waves of sufficient intensity are produced. The required intensity might be achieved by pulsing a coil and/or proper focusing of the waves; in this way fusion plasmas might be heated with the heating localized to the central plasma region.

This mechanism can also be invoked to interpret space plasma problems, such as the situation near the bow shock of the Earth in the solar wind, where Alfvén waves and highly energetic ions are observed. Some of these ions are detected in the upstream region (i.e., in the solar wind). There have recently been a number of shock simulations[5-7]; we have also begun simulations in this area. Applications to solar and astrophysical problems (e.g., ejection of plasma in solar flares) can be also considered. Details of our studies of some of these problems will be presented in a longer paper elsewhere.

We would like to thank Jean-Noel Leboeuf for his help and Chih-Chien Lin for supplying the computer code. This work was supported by U. S. Department of Energy Contract No. DOE DE-AM03-76SF00010 PA 26, Task VI B, and by U. S. National Science Foundation Contract No. ATM 79-26492.

---

[a]On leave from Centre de Recherches en Physique de l'Environnement Terrestre et Planetaire/Centre National d'Etudes des Telecommunications, F-92131 Issy-les-Moulineaux, France.

[b]Present address: Department 72-30, Building 311, Plant B6, Lockheed-California Company, P.O. Box 551, Burbank, Cal. 91520.

[c]On leave from the Institute of Plasma Physics, Nagoya University, Nagoya 464, Japan.

[1]P. L. Auer, R. W. Kilb, and W. F. Crevier, J. Geophys. Res. 76, 2927 (1971).

[2]D. Biskamp and H. Welter, Nucl. Fusion 12, 663 (1972).

[3]D. Sherwell and R. A. Cairns, J. Plasma Phys. 17, 265 (1976).

[4]D. L. Morse, J. Geophys. Res. 81, 6126 (1976).

[5]M. M. Leroy, C. C. Goodrich, D. Winske, C. S. Wu, and K. Papadopoulos, Geophys. Res. Lett. 8, 1269 (1982).

[6]M. M. Leroy, D. Winske, C. C. Goodrich, C. S. Wu, and K. Papadopoulos, J. Geophys. Lett. 87, 5081 (1982).

[7]D. W. Forslund, K. Quest, J. U. Brackbill, and K. Lee, to be published.

[8]R. Sagdeev and V. Shapiro, Pis'ma Zh. Eksp. Teor. Fiz. 17, 389 (1973) [JETP Lett. 17, 279 (1973)].

[9]R. Sugihara and Y. Midzuno, J. Phys. Soc. Jpn. 47, 1290 (1979).

[10]J. M. Dawson, V. K. Decyk, Robert W. Huff, I. Jechart, T. Katsouleas, J. N. Leboeuf, B. Lembege, R. Martinez, Y. Ohsawa, and S. Ratliff, Phys. Rev. Lett. 50, 1455 (1983).

[11]A. B. Langdon and B. F. Lasinski, in *Methods of Computational Physics*, edited by B. Alder *et al.* (Academic, New York, 1976), Vol. 16, p. 300.

[12]A. T. Lin, J. M. Dawson, and H. Okuda, Phys. Fluids 17, 1995 (1974).

[13]C. F. F. Karney, Phys. Fluids 21, 1584 (1978), and 22, 2188 (1979).